Total and isomeric-state cross sections for the ^{76}Ge$(n,2n)^{75}$Ge reaction from threshold to 14.8 MeV

Megha Bhike,* Krishichayan, and W. Tornow
Department of Physics, Duke University, Durham, North Carolina 27708, USA
and Triangle Universities Nuclear Laboratory, Durham, North Carolina 27708, USA
(Received 3 January 2017; revised manuscript received 20 March 2017; published 4 May 2017)

The cross sections for the reaction ^{76}Ge$(n,2n)^{75}$Ge to both the isomeric state and the ground state of ^{75}Ge have been measured with the activation method between 10 and 15 MeV in small energy steps to help resolve inconsistencies in the existing database. The ^{197}Au$(n,2n)^{196}$Au reaction with its known cross section was used for normalization of the data, which are compared to experimental and evaluated data of the EXFOR, EAF, JENDL, ENDF, and TENDL libraries. Model calculations using the TALYS-1.8 code are presented which also allow for the extrapolation to higher neutron energies. The data are important to estimate potential neutron-induced backgrounds in currently running large-scale experiments aimed at the discovery of neutrinoless $\beta\beta$ decay of ^{76}Ge.

DOI: 10.1103/PhysRevC.95.054605

I. INTRODUCTION

The germanium detector array (GERDA) and MAJORANA collaborations use germanium-diode detectors in their searches for neutrinoless $\beta\beta$ decay ($0\nu\beta\beta$) of ^{76}Ge [1,2]. These highly enriched detectors (86% ^{76}Ge, 14% ^{74}Ge) serve as both source and detector. Common to all $0\nu\beta\beta$-decay searches is the requirement that background events in the energy region of interest, a narrow energy band centered at the Q value for $0\nu\beta\beta$ decay, must be extremely small. To help achieve this goal, the experiments are being performed deep underground, resulting in a substantial reduction of cosmogenic background. However, some of the remaining muons may interact with nuclei in the vicinity of the detector or within the detector itself, producing so-called spallation neutrons. During the slowing-down process of these neutrons, (n,xn) reactions with $n \geqslant 2$ play an important role. These reactions tend to multiply the incident spallation neutron yield by typically 1 order of magnitude for a 100-MeV spallation neutron.

The ^{76}Ge$(n,2n)^{75}$Ge reaction is of special importance because its $(n,2n)$ cross section is of hundreds of millibarns. A partial level scheme of ^{75}Ge and its β-decay daughter ^{75}As is shown in Fig. 1. The ^{76}Ge$(n,2n)^{75}$Ge reaction populates the $7/2^+$ isomeric state of ^{75}Ge at 139.7 keV, which either decays via an isomeric transition (IT) to the $1/2^-$ ground state with $T_{1/2} = 47.7$ s and a branching ratio of 99.97% or via β decay to ^{75}As with a branching ratio of 0.03%. The ground state of ^{75}Ge in turn β decays with $T_{1/2} = 82.78$ min to ^{75}As.

In this work, we report on the activation cross sections for the reactions ^{76}Ge$(n,2n)^{75m}$Ge (isomeric state), ^{76}Ge$(n,2n)^{75}$Ge (total), and ^{76}Ge$(n,2n)^{75g}$Ge (ground state) at 11 neutron energies from threshold to 14.8 MeV. The associated Q values are -9.55 and -9.69 MeV, respectively. The results are compared to estimates of recent evaluated data libraries and data from the literature. In addition, we have compared the measured cross-section data of these reactions with theoretical model calculations performed with the TALYS code (version 1.8) [4] in the neutron energy range of 10 to 16 MeV. The calculations were made using different level-density options to match the cross-section data measured in the present work.

II. EXPERIMENT AND PROCEDURE

The cross-section measurements were performed using the neutron-activation technique. Irradiations were carried out in the 10-MV FN Tandem Van de Graaff Accelerator at the Triangle Universities Nuclear Laboratory (TUNL) using two different neutron source reactions. First, the ^{2}H$(d,n)^3$He reaction ($Q = 3.269$ MeV) was used to produce quasimonoenergetic neutrons between 9.9 and 14.5 MeV employing a deuterium gas target cell. The gas pressure was adjusted to 4 atm to provide the desired neutron energy spread in the energy range investigated. Typically the neutron energy spread was ± 150 keV at 0°. Second, at 14.8 MeV, the ^{3}H$(d,n)^4$He reaction ($Q = 17.59$ MeV) was employed by replacing the deuterium gas cell by a tritiated target assembly. It consisted of a 2-mg/cm^2-thick titanium layer loaded with 2.5 Ci of tritium and evaporated onto a 0.4-mm-thick copper disk. A metallic germanium slab 10 mm × 10 mm in area and with a thickness of 2 mm (resulting in a mass of about 1.5 g) with the same isotopic composition as that of the enriched high-purity germanium (HPGe) detectors used by the GERDA and MAJORANA Collaborations was supported by a thin plastic foil and positioned 1.9 cm from the end of the deuterium gas cell at 0° relative to the direction of the incident deuteron beam (see Fig. 1 of Ref. [5]). A total of three slabs were used one at a time during the course of the measurements to optimize the efficiency of our irradiation and counting procedure. The deuteron beam current was typically 2 μA.

To normalize the neutron flux at the Ge slab position, high-purity Au foils of the same area and thickness of 0.025 mm were placed on the front and backside of the Ge slabs, enabling us to use the ^{197}Au$(n,2n)^{196}$Au reaction with $T_{1/2} = 6.17$ days, $E_\gamma = 355.73$ keV, and $I_\gamma = 87\%$ as the monitor reaction. The neutron-activation cross-section data for this reaction were obtained from Ref. [6]. The average

*megha@tunl.duke.edu

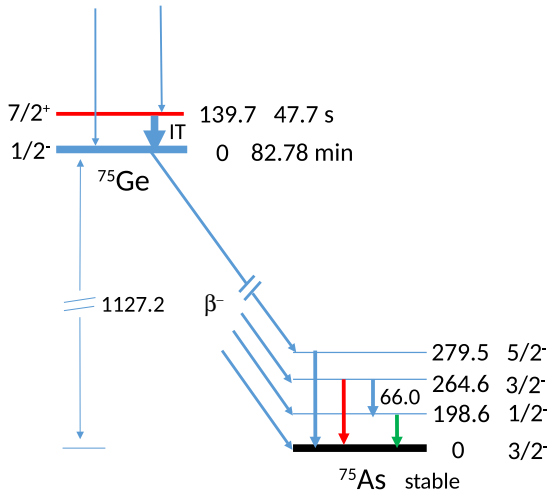

FIG. 1. Partial level scheme relevant to the ^{76}Ge$(n,2n)^{75m}$Ge and ^{76}Ge$(n,2n)^{75}$Ge reactions. All energies are given in keV. Data are taken from Ref. [3].

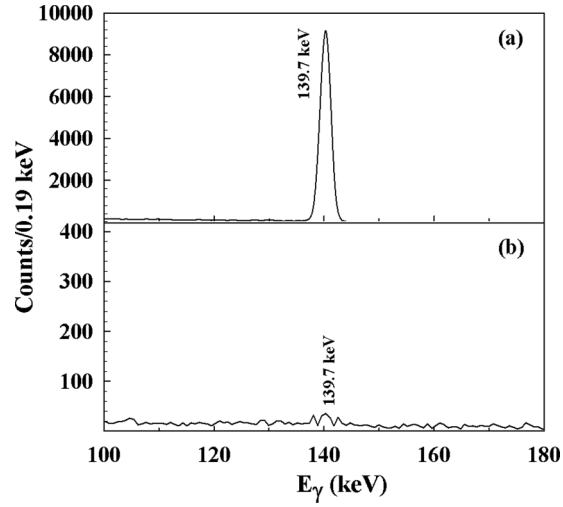

FIG. 2. (a) ^{75}Ge γ-ray line at 139.7 keV measured for 30 s with a HPGe detector starting 40 s after the 3-min irradiation time of ^{76}Ge with 12.87-MeV neutrons. (b) Same as panel (a), but with a starting time of 3.5 min after irradiation.

neutron flux produced at the Ge slab position ranged from 1.4×10^7 to 4.4×10^7 $n/(\mathrm{cm}^2\,\mathrm{s})$. A 1.5 in. $\times$ 1.5 in. BC-501A based neutron detector was placed at 0° relative to the incident deuteron beam. During irradiation, the detector operated in the multichannel-scaling acquisition mode to record the time profile of the neutron flux, allowing us to make off-line corrections for any beam current variation.

Because of the high thresholds of the ^{76}Ge$(n,2n)^{75}$Ge and ^{76}Ge$(n,2n)^{75m}$Ge reactions, and the gap of about 5.5 MeV between the energy of the monoenergetic neutrons of the ^{2}H$(d,n)^3$He reaction and the maximum energy of the breakup continuum, the $(n,2n)$ reactions are not sensitive to breakup neutrons in the energy range studied in the present work.

High-resolution γ-ray detection systems located at TUNL's low background counting facility were used to record γ-ray spectroscopy data off-line for the irradiated samples and monitors foils. Two 60% HPGe detectors combined with a Canberra Multiport II multichannel analyzer and a 16-K analog-to-digital converter, supported by the Genie 2000 data-acquistion system, were employed. These detectors were properly shielded with lead blocks to reduce the contribution of natural radioactivity from the environment. The sample activities were determined using the counts in the full-energy peak of the γ-ray transition. For this it was important to know the absolute photopeak efficiency and the energy calibration. For energy and efficiency calibration, a mixed source consisting of the isotopes ^{241}Am ($E_\gamma = 59.5$ keV), ^{109}Cd ($E_\gamma = 88$ keV), ^{57}Co ($E_\gamma = 122.1$ keV), ^{139}Cs ($E_\gamma = 165.9$ keV), ^{203}Hg ($E_\gamma = 279.2$ keV), ^{113}Sn ($E_\gamma = 391.7$ keV), ^{134}Cs ($E_\gamma = 604.7$ keV), ^{137}Cs ($E_\gamma = 661.7$ keV), ^{54}Mn ($E_\gamma = 834.8$ keV), ^{65}Zn ($E_\gamma = 1115.5$ keV), and ^{88}Y ($E_\gamma = 1836.1$ keV) was used. The energy resolution was found to be $\sim$1.8 keV for 1836.2-keV γ rays emitted from ^{88}Y. The residual activity of samples and monitor foils was counted at a distance of 5 cm from the center of the detector window. The choice of this distance was the result of a compromise between assuring an acceptable count rate and reducing coincidence summing effects. Prior to irradiation, background measurements were performed with nonirradiated Ge-Au foils to check for any interference in the pulse-height region of interest. The induced activities in the germanium samples were determined by measuring the γ rays associated with the decay of ^{75m}Ge and ^{75}Ge at 139.7 keV (39.51%) and 264.6 keV (11.4%), respectively.

Typical spectra are shown in Figs. 2(a) and 2(b) for the 139.7-keV transition recorded 40 s and 3.5 min after the end of irradiation, respectively. Figures 3(a) and 3(b) present similar spectra for the 198.6- and 264.6-keV transitions of interest. The peak-area analysis was done with the program TV [7]. For the activity determination, half-lives, emission probability, γ-ray attenuation, spatial difference of the γ-ray

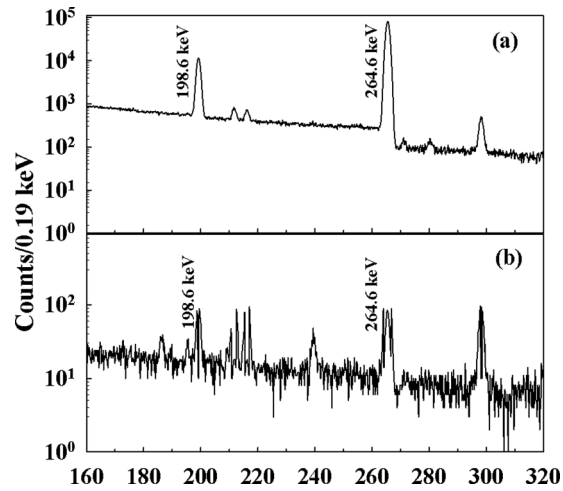

FIG. 3. (a) ^{75}As γ-ray lines at 198.6 and 264.6 keV measured for 2 h with a HPGe detector starting 0.3 h after the 1-h irradiation time of ^{76}Ge with 12.87-MeV neutrons. (b) Same as panel (a), but with a starting time of 10.5 h after irradiation.

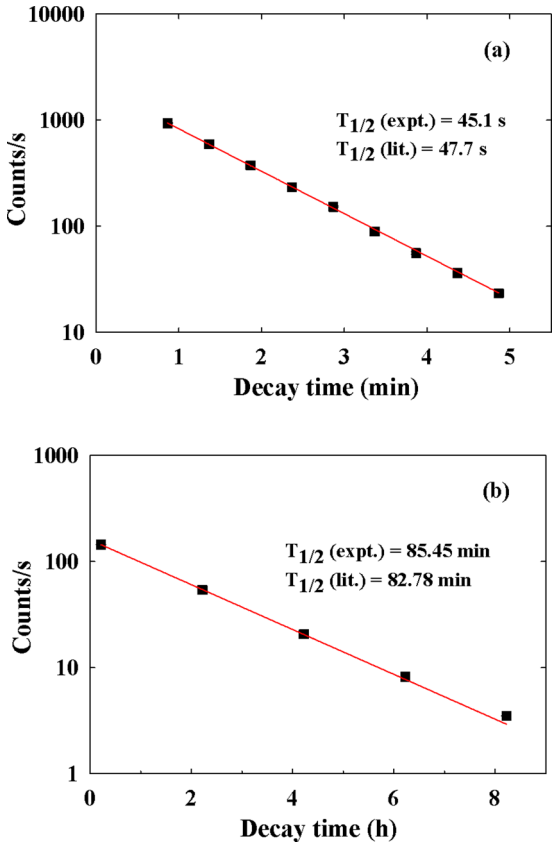

FIG. 4. Decay curves for (a) the 139.7-keV γ-ray line of ^{75m}Ge and (b) the 264.6-keV γ-ray line of ^{75}As obtained after irradiation with $E_n = 12.87$ MeV neutrons.

efficiency, and coincidence-summing corrections were taken into account. The decay data for both ^{75}Ge and ^{196}Au used in the analysis were taken from Ref. [3].

For the study of the ^{76}Ge$(n,2n)^{75m}$Ge reaction, a HPGe detector was mounted just outside of the target room to limit the time between irradiation and counting to typically 20 s. The sample was irradiated for three half-lives and the induced γ-ray activity of the 139.7-keV transition from the ^{75m}Ge decay was measured for a period of ten half-lives. Figures 4(a) and 4(b) show the intensities of both the 139.7- and 264.6-keV γ rays as a function of cooling time after irradiation.

The neutron fluence and cross-section values were derived using the well-known activation formula, closely following the procedure explained in Ref. [8]. The yields were corrected for dead time, γ-ray emission probability, γ-ray self-absorption including the size and shape of the samples and monitor foils, efficiency of the detector, time-dependence of the neutron flux, and source-size geometry.

III. RESULTS

The cross-section values measured in the present work along with their uncertainties are presented in Table I. The first column shows the neutron energy and its energy spread. The second column gives the ^{197}Au$(n,2n)^{196}$Au reaction cross-section values used to calculate the neutron flux. Columns 3 and 4 represent the cross-section results σ_m and σ_t for the reactions ^{76}Ge$(n,2n)^{75m}$Ge and ^{76}Ge$(n,2n)^{75}$Ge, respectively. To determine the $(n,2n)$ cross section σ_g to the ground state, the relation $\sigma_g = \sigma_t - \sigma_m$ was used. This cross section is shown in column 5. Finally, column 6 gives the isomeric- to ground-state cross-section ratio σ_m/σ_g. As a by-product, the ^{74}Ge$(n,\alpha)^{71m}$Zn cross section was obtained at 14.8 MeV and found to be 3.24 ± 0.17 mb, in good agreement with the previous datum of Ref. [9]. Because of unfavorable threshold, decay-time, and γ-ray energy values, other neutron-induced reaction cross-section determinations on ^{74}Ge and ^{76}Ge were not attempted in the present work.

The sources of errors considered in the activation measurements are shown in Table II: nuclear constants (half-life, γ-ray intensities), instrumental factors (time of irradiation, cooling, and measurements), and uncertainties related to the determination of the correction factors. The uncertainties of the measured cross-section data vary from 5.2% to 8.3%. By considering the uncertainities involved in the measurement of each parameter, the total uncertainty was obtained by taking the square root of the sum of the squares of the individual uncertainties.

TABLE I. Measured cross sections and deduced isomeric yield ratio obtained in the present work at neutron energies from $E_n = 9.9$ to 14.8 MeV.

$E_n \pm \Delta E_n$ (MeV)	σ_{mon} (mb)	^{76}Ge$(n,2n)^{75m}$Ge (mb)	^{76}Ge$(n,2n)^{75}$Ge (mb)	^{76}Ge$(n,2n)^{75g}$Ge (mb)	σ_m/σ_g
9.90±0.11	964.21 ± 29.50	22.14 ± 1.84	44.91 ± 2.59	22.77 ± 2.30	0.97 ± 0.13
10.39±0.14	1411.41 ± 39.52	124.85 ± 7.12	214.30 ± 12.22	89.45 ± 7.21	1.40 ± 0.14
10.89±0.14	1701.31 ± 44.06	226.25 ± 13.21	355.81 ± 18.46	129.56 ± 10.12	1.75 ± 0.17
11.39±0.14	1573.60 ± 42.30	360.94 ± 22.88	528.75 ± 30.23	167.81 ± 14.33	2.15 ± 0.23
11.88±0.13	1706.34 ± 44.19	446.51 ± 28.58	660.35 ± 33.82	213.84 ± 17.53	2.10 ± 0.22
12.38±0.15	1828.14 ± 44.79	535.83 ± 35.36	800.07 ± 59.32	264.24 ± 26.23	2.03 ± 0.24
12.87±0.15	1938.13 ± 44.00	598.72 ± 39.64	881.83 ± 65.38	283.11 ± 28.14	2.11 ± 0.25
13.37±0.15	2038.87 ± 37.92	640.87 ± 43.32	941.42 ± 45.02	300.55 ± 24.89	2.13 ± 0.23
13.87±0.07	2116.77 ± 26.46	696.85 ± 42.09	1026.67 ± 46.78	329.82 ± 24.95	2.11 ± 0.21
14.36±0.11	2153.29 ± 24.12	740.11 ± 43.67	1070.21 ± 53.18	330.10 ± 25.46	2.24 ± 0.22
14.80±0.07	2164.20 ± 22.83	754.56 ± 46.86	1090.26 ± 54.71	335.70 ± 26.80	2.25 ± 0.23

TABLE II. Uncertainty budget for the ^{76}Ge$(n,2n)^{75}$Ge, ^{76}Ge$(n,2n)^{75m}$Ge, and monitor reaction cross-section values.

Parameter	Ge (%)	Monitor (%)
Photopeak area	0.1–2.48	0.36–6.32
Reference cross sections		1.05–3.06
Detector efficiency	2.30–5.92	0.62–5.30
Source geometry and self-absorption of γ rays	<0.2	<0.2
Half-life	<1.1	0.01
γ-ray intensity	—	—
Irradiation time	<1	<1
Decay time	<1	<1
Counting time	<1	<1
Neutron-flux correction	—	<2
Neutron-flux fluctuation	<1	<1

The experimental data obtained in the present work (downward looking triangles) are shown in Figs. 5 and 6 along with values from the literature and results from the available comprehensive evaluations: TENDL-2014 [18], EAF-2010 [19], JENDL-4.0 [20], and ENDF/B-VII.1 [21] databases. The results shown in Fig 5 reveal that our results for the ^{76}Ge$(n,2n)^{75m}$Ge reaction above 13 MeV favor the lower cluster of the previous experimental data [10,11,13,14,17], while the data of Bormann *et al.* [16], Kasugai *et al.* [12], and the Hlavac *et al.* [15] provide larger cross-section values. Our data below 13 MeV are the first data in this energy range. They give an accurate determination of the cross section in the important energy region above the $(n,2n)$ threshold. The TENDL-2014 predictions are in much better agreement with the present data than the EAF-2010 evaluation, which favors the upper cluster of the previously available experimental data.

Inspecting Fig. 6, we note that our data for the ^{76}Ge$(n,2n)^{75}$Ge reaction in the 14-MeV region are in good agreement with the lower set of the previous cross-section data. At lower energies the present data confirm the energy dependence established by the two data points of Ref. [28] near 12.5 and 13 MeV and the five data points of Refs. [11,22] below 11.5 MeV. Because the model calculation TENDL-2014 and the evaluations JENDL-4.0 and ENDF/B-VII.1 are trying to reproduce the average of the data in the 14-MeV energy region, they clearly overestimate the ^{76}Ge$(n,2n)^{75}$Ge cross-section data in the 11- to 12.5-MeV energy range. Figures 7 and 8 show the measured cross-section data in comparison with the calculations using the nuclear-model code TALYS (for explantion of curves see Sec. IV). Our results for the deduced cross section σ_g and the isomeric- to ground-state ratio σ_m/σ_g are shown in Figs. 9 and 10 (see Sec. IV).

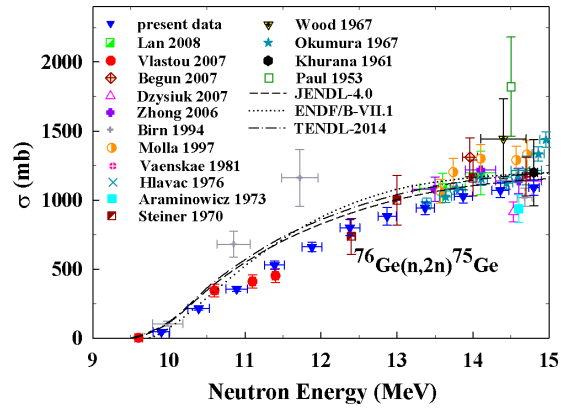

FIG. 6. Cross-section results for the ^{76}Ge$(n,2n)^{75}$Ge reaction compared with results from earlier measurements [11,13,15,22–32], the model calculation TENDL-2014, and the JENDL-4.0 [20] and ENDF/B-VII.1 [21] evaluations.

IV. NUCLEAR-MODEL CALCULATIONS

The cross sections for the ^{76}Ge$(n,2n)^{75m}$Ge, ^{76}Ge$(n,2n)^{75}$Ge, and ^{76}Ge$(n,2n)^{75g}$Ge reactions were calculated in the neutron energy range from 9 to 16 MeV using the recent version (version 1.8) of the nuclear-model code TALYS [4]. In the present work the calculations have been

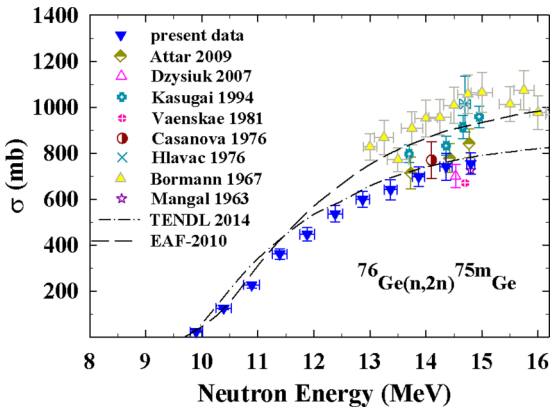

FIG. 5. Experimental results for the ^{76}Ge$(n,2n)^{75m}$Ge reaction compared with results from earlier measurements [10–17], the model calculation TENDL-2014 [18], and the EAF-2010 [19] evaluation.

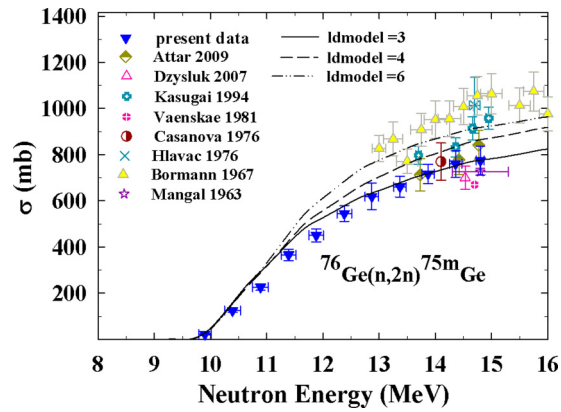

FIG. 7. Comparison of cross-section data [10–17] and TALYS calculations for the ^{76}Ge$(n,2n)^{75m}$Ge reaction using different level-density choices (see text). Our data are best described by the generalized superfluid model.

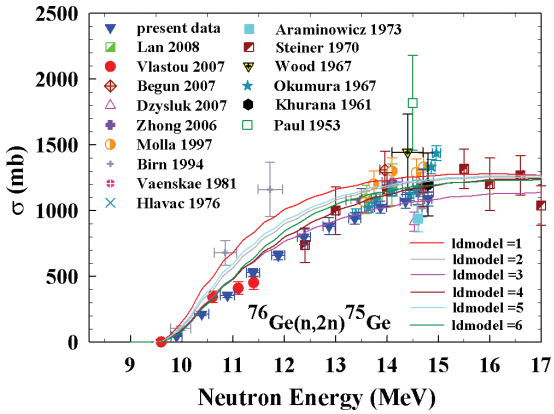

FIG. 8. Comparison of cross-section data [11,13,15,22–32] and TALYS calculations for the ^{76}Ge$(n,2n)^{75}$Ge reaction using different level-density choices (see text). Our data are best described by the generalized superfluid model.

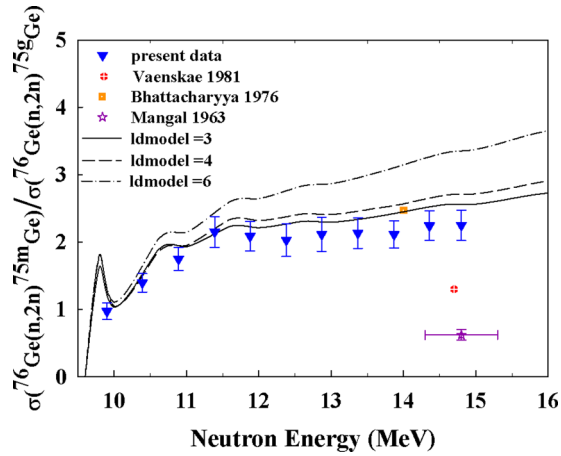

FIG. 10. Comparison of the energy dependence of the measured isomeric- to ground-state cross-section ratio for the ^{76}Ge$(n,2n)^{75}$Ge reaction with the predictions obtained using the TALYS code and with the existing previous measurements [13,17,33].

performed mainly with input parameters given by default settings in TALYS. However, one exception deals with the nuclear level density. Here, particular models were used to investigate their sensitivity.

The level density is an essential ingredient for calculation of reaction cross sections. It is a key parameter in any statistical model calculation at excitation energies where discrete level information is not available or incomplete. The most important step for determining a reliable theoretical prediction of cross sections, energy spectra, angular distributions, and other nuclear reaction observables is to use the correct level density together with the appropriate optical-model potential parameters. In TALYS-1.8, the level density can be calculated via six different choices, corresponding to the input parameter ldmodel equal to 1 to 6. The three phenomenological and the three microscopic options for level densities are as follows: ldmodel = 1, constant temperature plus Fermi gas model; ldmodel = 2, back-shifted Fermi gas model; ldmodel = 3, generalized super-fluid model; ldmodel = 4, microscopic level densities (Skyme force) from Goriely's tables; ldmodel = 5, microscopic level densities (Skyme force) from Hilaire's combinatorial tables; ldmodel = 6, microscopic level densitites (temperature-dependent Hartree-Fock-Bogoliubov, Gogny force) from Hilaire's combinatorial tables.

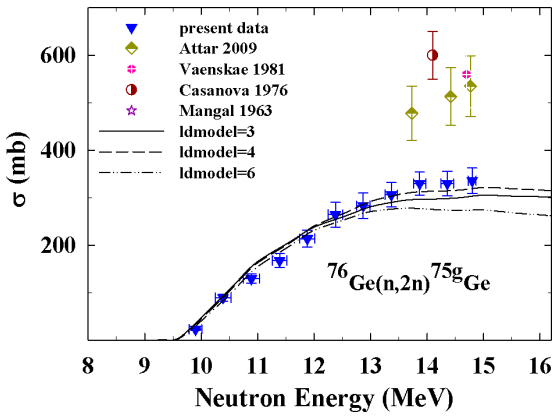

FIG. 9. Comparison of cross-section data [10,13,14] and TALYS calculations for the ^{76}Ge$(n,2n)^{75g}$Ge reaction using different level-density choices (see text). Our data are best described by the generalized superfluid model.

Moreover, in these TALYS calculations, for each level-density choice, the default proton and neutron optical-model potentials using the local and global parametrization of Koning and Delaroche can be applied [34]. These potentials provide the necessary reaction cross sections and transmission coefficients for the statistical model calculations. The TALYS nuclear structure database has been generated from the Reference Input Parameter Library [35]. The Hauser-Feshbach model is used for the calculation of the compound-nucleus contribution [36]. In addition, the pre-equilibrium reactions were included via the two-component exciton model of Kalbach [37].

A comparison of experimental data for the reactions of interest with predictions of the TALYS-1.8 code utilizing different level-density model options is presented in Figs. 7–10. It can be clearly seen that for our experimental results the best agreement is achieved using the calculations with ldmodel = 3. For completeness, Fig. 8 shows calculations with all the level-density options provided with the TALYS-1.8 code, in contrast to Figs. 7, 9, and 10, where only a subset of level-density choices are considered.

V. CONCLUSION

The total and isomeric-state cross sections of the reaction ^{76}Ge$(n,2n)^{75}$Ge were measured from threshold to 14.8 MeV to guide evaluations and model calculations to provide reliable cross-section data throughout the energy range of interest for tracking neutrons in future large-scale HPGe detectors currently envisioned for searches of $0\nu\beta\beta$ of ^{76}Ge. Neutron-induced background reactions are a major concern because they have the potential to mimic the signal of interest. Our measured cross-section data follow the trend of the few previous data below 13 MeV, but are lower in magnitude than

most of the data in the heavily researched 14-MeV energy range, resulting in evaluations and the model calculation TENDL-2014 to miss our data for energies above 11 MeV. Previous data for the isomeric-state cross section do not exist below 13 MeV. However, above this energy our data favor the lower band of the available data. Our TALYS calculations performed with the level density of the generalized superfluid model give an overall satisfactory description of the measured total and isomeric-state cross section and the deduced ground-state cross section of the ^{76}Ge$(n,2n)^{75}$Ge reaction.

ACKNOWLEDGMENTS

This work was supported in part by the U.S. Department of Energy, Office of Nuclear Physics, under Grant No. DE-FG02-97ER41033.

[1] M. Agostini *et al.*, Phys. Rev. Lett. **111**, 122503 (2013).
[2] M. Abgrall *et al.*, Adv. High Energy Phys. **2014**, 1 (2014).
[3] http://www.nndc.bnl.gov/nudat2/.
[4] A. J. Koning, S. Hilaire, and M. C. Duijvestijn, TALYS-1.0, in *Proceedings of the International Conference on Nuclear Data for Science and Technology - ND2007, April 22–27, 2007, Nice, France*, edited by O. Bersillon, F. Gunsing, E. Bauge, R. Jacqmin, and S. Leray (EDP Sciences, Les Ulis, France, 2008), pp. 211–214.
[5] M. Bhike, B. Fallin, Krishichayan, and W. Tornow, Phys. Lett. B **741**, 150 (2015).
[6] K. I. Zolotarev *et al.*, INDC Report No. (NDS)-0526, 2008.
[7] J. Theuerkauf, S. Esser, S. Krink, M. Luig, N. Nicolay, O. Stauch, and H. Wolters, Program TV, Institute for Nuclear Physics, University of Cologne, 1993 (unpublished).
[8] M. Bhike and W. Tornow, Phys. Rev. C **89**, 031602(R) (2014).
[9] G. P. Vinitskaya, V. N. Levkovskiy, V. V. Sokol'skiy, and I. V. Kazachevskiy, Yad. Fiz. **6**, 240 (1967).
[10] F. M. D. Attar, S. D. Dhole, S. Kailas, and V. N. Bhoraskar, Nucl. Phys. A **828**, 253 (2009).
[11] R. Vlastou *et al.*, J. Radioanal. Nucl. Chem. **272**, 219 (2007).
[12] Y. Kasugai, H. Yamamoto, K. Kawade, Y. Ikeda, Y. Uno, and H. Maekawa, in *Proceedings of Conference on Nuclear Data for Science and Technology, Gatlinburg, Tennessee*, 1994, p. 935.
[13] R. Vaenskae and R. Rieppo, Nucl. Instrum. Methods **179**, 525 (1981).
[14] J. L. Casanova and M. L. Sanchez, An. Fis. Quim. **72**, 186 (1976).
[15] S. Hlavac, J. Kristiak, P. Oblozinsky, and I. Turzo, Acta Phys. Slovaca **26**, 64 (1976).
[16] M. Bormann, C. Abels, W. Carstens, and I. Riehle, Report from Euratom-countries + Euratom to EANDC No. 76, 1967, p. 51.
[17] S. K. Mangal and P. S. Gill, Nucl. Phys. **49**, 510 (1963).
[18] A. J. Koning and D. Rochman, Nucl. Data Sheets **113**, 2841 (2012).
[19] J.-Ch. Sublet, L. W. Packer, J. Kopecky *et al.*, The European Activation File: EAF-2010 Neutron-induced Cross Section Library, EASY Documentation Series CCFE-R (10) 05, April 2010.
[20] K. Shibata *et al.*, Nucl. Sci. Technol. **48**, 1 (2011).
[21] M. B. Chadwick *et al.*, Nucl. Data Sheets **112**, 2887 (2011).
[22] C. Lan, X. Xu, K. Fang, G. Liu, X. Kong, R. Liu, and L. Jiang, Ann. Nucl. Energy **35**, 2105 (2008).
[23] S. V. Begun, O. G. Druzheruchenko, O. O. Pupirina, and V. K. Tarakanov, arXiv:nucl-ex/0701039.
[24] P. Zhong-Sheng, G. Qiu-Yun, M. Jun, and Y. Dong, High Energy Phys. Nucl. Phys. Chinese edition **30**, 1171 (2006).
[25] N. I. Molla, R. U. Miah, S. Basunia, S. M. Hossain, and M. Rahman, in *Proceeding of Conference on Nuclear Data for Science and Technology, Trieste, Italy*, 1997, Vol. 1, p. 517.
[26] I. Birn, S. M. Qaim, B. Strohmaier, and H. Freiesleben, Nucl. Sci. Eng. **116**, 125 (1994).
[27] J. Araminowicz and J. Dresler, Progress Report: Inst. Badan Jadr. (Nuclear Research), Sierk + Warsaw, Report No. 1464, 1973, p. 14.
[28] E. Steiner, P. Huber, W. Salathe, and R. Wagner, Helv. Phys. Acta **43**, 17 (1970).
[29] R. E. Wood, W. S. Cook, J. R. Goodgame, and R. W. Fink, Phys. Rev. **154**, 1108 (1967).
[30] S. Okumura, Nucl. Phys. A **93**, 74 (1967).
[31] C. S. Khurana and H. S. Hans, Nucl. Phys. **28**, 560 (1961).
[32] E. B. Paul and R. L. Clarke, Can. J. Phys. **31**, 267 (1953).
[33] P. Bhattacharyya, R. K. Chattopadhayay, B. Sethi, A. Basu, and J. M. Chatterjee-Das, Il Nuovo Cimento A **31**, 519 (1976).
[34] A. J. Koning and J. P. Delaroche, Nucl. Phys. A **713**, 231 (2003).
[35] R. Capote *et al.*, Nucl. Data Sheets **110**, 3107 (2009).
[36] W. Hauser and H. Feshbach, Phys. Rev. **87**, 366 (1952).
[37] C. Kalbach, Phy. Rev. C **33**, 818 (1986).